Prospect for room temperature tunneling anisotropic magnetoresistance effect: Density of states anisotropies in CoPt systems

A. B. Shick,[1] F. Máca,[1] J. Mašek,[1] and T. Jungwirth[2,3]

[1]*Institute of Physics ASCR, Na Slovance 2, 182 21 Praha 8, Czech Republic*
[2]*Institute of Physics ASCR, Cukrovarnická 10, 162 53 Praha 6, Czech Republic*
[3]*School of Physics and Astronomy, University of Nottingham, University Park, Nottingham NG7 2RD, United Kingdom*
(Received 18 October 2005; published 25 January 2006)

Tunneling anisotropic magnetoresistance (TAMR) effect, discovered recently in (Ga,Mn)As ferromagnetic semiconductors, arises from spin-orbit coupling and reflects the dependence of the tunneling density of states in a ferromagnetic layer on orientation of the magnetic moment. Based on *ab initio* relativistic calculations of the anisotropy in the density of states we predict sizable TAMR effects in room-temperature metallic ferromagnets. This opens the prospect for new spintronic devices with a simpler geometry as these do not require antiferromagnetically coupled contacts on either side of the tunnel junction. We focus on several model systems ranging from simple hcp-Co to more complex ferromagnetic structures with enhanced spin-orbit coupling, namely bulk and thin film $L1_0$-CoPt ordered alloys and a monatomic-Co chain at a Pt surface step edge. Reliability of the predicted density of states anisotropies is confirmed by comparing quantitatively our *ab initio* results for the magnetocrystalline anisotropies in these systems with experimental data.

The area of condensed matter research that aims at exploiting synergies of magnetic and semiconducting properties in solid state systems has served as an important test bed for understanding basic physics and discovering new applications in spintronics.[1,2] The anomalous Hall effect and the tunneling anisotropic magnetoresistance (TAMR) studies are two examples of the research that provided main motivation for the work presented here. The former study demonstrated[3–7] that a successful theory of the anomalous Hall effect in (Ga,Mn)As ferromagnetic semiconductors, based on spin-orbit (SO) coupling effects present in the band structure of Bloch states, can be directly applied to conventional metallic ferromagnets such as Fe, and describe quantitatively this fundamental transport coefficient. The TAMR effect[8] is an offspring of attempts to develop hybrid metal-semiconductor spin-valve devices which revealed that a spin-valve-like response can be achieved without the seemingly fundamental switching sequence between parallel and antiparallel magnetizations in two ferromagnetic contacts with different coercivities. Instead, a single ferromagnetic material with SO interaction is sufficient for realizing the sensing or memory functionality through TAMR whose phenomenology is even richer than that of conventional giant magnetoresistance or tunneling magnetoresistance effects. For example, both lower and higher resistance states can be obtained at saturation depending on the external magnetic field orientation, i.e., the TAMR device can act as a sensor of the absolute direction of the external field.[9]

The TAMR was discovered in a $(Ga,Mn)As/AlO_x/Au$ stack[8] and confirmed by subsequent experiments in (Ga,Mn)As based vertical[9] and planar[10] tunnel devices. The former experiment underlined the importance of high quality interfaces and barrier materials for the magnitude of the effect. The lithographically defined planar nanodevice allowed to demonstrate a direct link between the TAMR in the tunneling nanoconstriction and normal anisotropic magnetore-sistance in the ferromagnetic lead. Since the latter effect also originates from SO coupling and has been observed in many metallic systems the work suggests that the TAMR has been overlooked in conventional room temperature ferromagnets. To explore this possibility we follow a theoretical strategy applied previously to (Ga,Mn)As TAMR devices which is based on calculating tunneling density of states (DOS) anisotropies in the ferromagnet with respect to the orientation of the magnetic moment and which assumes a proportionality between the DOS and tunneling conductance anisotropies.

The paper is organized as follows: We start with a simple hcp-Co crystal as a benchmark material and then add to the complexities of the studied structures in order to enhance SO coupling related effects. The next system we explore is bulk $L1_0$-CoPt alloy.[11,12] Here Co produces large exchange splitting resulting in the Curie temperature of 750 K while the heavy elements of Pt substantially increase the strength of SO coupling in the band structure of the alloy. Effects of reduced dimensionality are explored in a thin $L1_0$-CoPt film and, reaching the ultimate nanoscale regime, in the monatomic-Co chain at Pt surface step edge.[13–15] An important part of the presented work is a simultaneous analysis of magnetocrystalline anisotropies in the studied structures. Given the predictive nature of our theoretical conclusions for tunneling DOS anisotropies, calculations of a physical quantity originating from the same SO coupled *ab initio* band structure and directly comparable to existing experimental data is particularly valuable. Magnetocrystalline anisotropies, and the derived magnetization reversals in external magnetic fields, are also important characteristics that define functionality of a TAMR device.

We use the relativistic version of the full-potential linearized augmented plane-wave method (FP-LAPW),[16] in which SO coupling is included in a self-consistent second-variational procedure.[17] The conventional (von Barth-Hedin)

TABLE I. DOS in hcp-Co and L1$_0$CoPt: Total integral DOS N_I (1/eV) and tunneling DOS N_T [eV(a.u.)^2] DOS at E_F for $\vec{M}_s \| x$ and z axes. For L1$_0$-CoPt film we show also layer- and spin-projected DOS. The k-space convergence achieved in the numerical calculations, using the smooth Fourier interpolation scheme (Ref. 19), gives error bars <1% for $N_I(x)$ in hcp-Co, <2.5% for N_T in hcp-Co, and <0.5% for $N_I(x)$ and N_T in L1$_0$ CoPt.

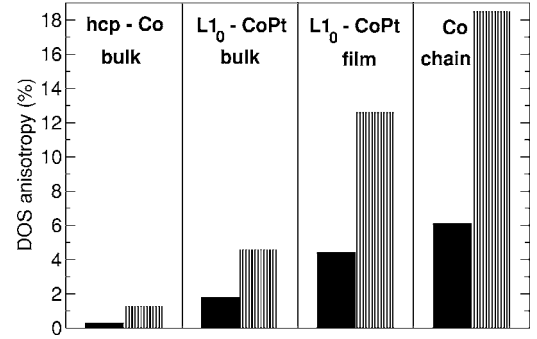| hcp-Co	$\vec{M}_S \| x$ axis	$\vec{M}_S \| z$ axis
N_I	1.999	2.004
N_T	6.780	6.696
L1$_0$-CoPt-bulk	$\vec{M}_S \| x$ axis	$\vec{M}_S \| z$ axis
N_I	2.091	2.055
N_T	10.709	11.205
L1$_0$-CoPt-film	$\vec{M}_S \| x$ axis	$\vec{M}_S \| z$ axis
N_I	13.310	12.745
	$N_I^\uparrow + N_I^\downarrow = N_I^{\text{tot}}$	$N_I^\uparrow + N_I^\downarrow = N_I^{\text{tot}}$
Pt surface	0.489+0.485=0.974	0.385+0.480=0.865
Co subsurface	0.231+1.637=1.868	0.187+1.615=1.802

FIG. 1. Bulk systems, integral (filled bars) and tunneling (half-filled bars) DOS anisotropy, $|N_{I(T)}(x) - N_{I(T)}(z)| / \min(N_{I(T)}(x), N_{I(T)}(z))$. L1$_0$-CoPt thin film, integral (filled bar) and Pt-surface (half-filled bar) DOS anisotropy. Monoatomic Co chain, $|N_I(x) - N_I(z)| / \min(N_I(x), N_I(z))$ for A-step (filled bar) and $|N_I(x) - N_I(y)| / \min(N_I(x), N_I(y))$ for B-step (half-filled bar).

local spin-density approximation is adopted, which is expected to be valid for itinerant metallic systems. The magnetic force theorem[18] is used to evaluate the DOS anisotropy and the magnetocrystalline anisotropy energy (MAE): starting from self-consistent charge and spin densities calculated for the magnetic moment M_S aligned along one of principal axes, the M_S is rotated and a single energy band calculation is performed for the new orientation of M_S. The DOS and magnetocrystalline anisotropies result from SO coupling induced changes in the band eigenvalues. Importantly, the same set of k-points must be used for the integration over the Brillouin zone (BZ) for accurate evaluation of the DOS anisotropy and of the MAE. Furthermore, in order to increase the accuracy in DOS evaluation, the smooth Fourier interpolation scheme of Pickett *et al.*[19] is used together with linear tetrahedron method.[20]

We start by investigating the possibility of TAMR in elemental transitional metal ferromagnets. Bulk hcp-Co is a theoretically well understood uniaxial ferromagnet with the MAE of 60 μeV per unit cell and the easy axis of magnetization along the z-[0001] crystallographic direction.[21] To evaluate the DOS anisotropy, we first performed the self-consistent FP-LAPW calculation of the band structure of hcp-Co using experimental lattice constant values and fixing M_S along the z-[0001] axis. The DOS anisotropy is obtained by rotating M_S from the z-[0001] axis to the in-plane x-[1000] axis. 1200 k-points were used for the BZ integration. The integral DOSs at the Fermi energy for M_S along the x-[1000] axis, $N_I(x)$, and z-[0001] axis, $N_I(z)$, are given in Table I. Corresponding DOS anisotropy defined as $|N_I(x) - N_I(z)| / \min(N_I(x), N_I(z))$ is plotted in Fig. 1 (see black bars). The integral DOS anisotropy $\sim$0.3% is relatively weak, similar to the weak magnetocrystalline anisotropy, which is a result of a small value of SO coupling

in elemental 3d-metals. Assuming high crystalline quality of an hcp-Co based TAMR device with a large degree of in-plane momentum conservation during the tunneling, we can improve our estimate of the effect by considering the tunneling DOS at the Fermi energy,[22] $N_T = 1/\Omega_{\text{BZ}} \int_{\text{BZ}} d^3k v_z^2(E_F) \delta[E(\vec{k}) - E_F]$, where $v_z = \partial E(\vec{k}) / \partial k_z$ is the group velocity component along the tunneling z-direction and E_F is the Fermi energy. The corresponding anisotropy (see blue bar in Fig. 1) is a factor of 4 larger than the anisotropy in N_I, which is a trend seen previously in the (Ga,Mn)As.[8] The 1.3% anisotropy in N_T suggests a measurable, albeit weak, TAMR effect even with a simple hcp-Co.

A natural recipe for enhancing the TAMR effect is by using ordered mixed crystals of magnetic 3d and nonmagnetic 5d transition metals. In these systems the magnetic atoms can produce large exchange fields polarizing the neighboring heavy elements with strong SO coupling. Pt is particularly favorable because of its large magnetic susceptibility. Here we consider the L1$_0$-CoPt alloy, which is known to have a strong MAE with the easy-axis aligned perpendicular to alternating Co and Pt metal layers.[11] The large anisotropy results from broken cubic symmetry in this layered alloy and from the presence of heavy elements of Pt, as explained above. Our previous relativistic FP-LAPW calculations[12] yield the MAE of 1.03 meV, in a very good agreement with experimental data.[11] DOS anisotropy calculations performed here follow the same numerical procedures as in Ref. 12. Starting from self-consistent calculations for M_S aligned along the z-[001] axis, we rotate M_S to the x-[110] direction and calculate the corresponding DOS. 952 k-points in the irreducible part of BZ (3584 k-points in full BZ) are used in these numerical simulations. As expected, both the N_I anisotropy of 1.8% and N_T anisotropy of 4.6% (see Table I and Fig. 1) in this mixed crystal are substantially larger than their hcp-Co counterparts.

So far we have demonstrated prospects of room temperature TAMR and confirmed expected trends in the TAMR with increasing strength of SO coupling in well understood conventional ferromagnets. In these bulk systems, *ab initio* relativistic calculations are known to provide accurate description of their properties, including the subtle, SO cou-

pling related magnetocrystalline anisotropy. The two model systems discussed in the following paragraphs allow us to take a different view of the DOS anisotropy which might be more closely related to the TAMR in real tunneling structures and, in the latter case, explores metallic TAMR in the ultimate nanoscale limit. Ferromagnetic electrodes in magnetic tunnel junctions are grown in thin films in which surfaces and/or interfaces effects are known to play an important role. To analyze these effects in our context we evaluate DOS anisotropies of a free-standing $L1_0$-CoPt film consisting of 5 Co and 6 Pt layers with the same interlayer distances as in the bulk. 400 k-points in the two-dimensional BZ were used in the numerical calculations. The resulting N_I anisotropy of the film is more than a factor of 2 larger than in the bulk $L1_0$-CoPt. Assuming a vacuum tunnel barrier and realizing that tunneling transport characteristics are dominated by properties of electronic states near the barrier, we can use the calculated DOS spatially resolved to individual layers to make a refined estimate of the TAMR effect in the $L1_0$-CoPt film. The partial DOS corresponding to surface Pt and subsurface Co monolayers are listed in Table I. The anisotropy in the DOS of the surface Pt layer is close to 13%. We note that the MAE per two-dimensional unit cell is about a factor of 5 larger than the anisotropy per three-dimensional unit cell in the bulk $L1_0$-CoPt. Recalling that our CoPt film has 5 Co and 6 Pt layers the MAE in the two structures are very similar. Since Curie temperatures in the film and bulk $L1_0$-CoPt can also be expected to be similar ($\sim$750 K) the magnetic tunnel junction based on thin film $L1_0$-CoPt is a good candidate for observing the TAMR effect at room temperature.

Recently, Gambardella *et al.*[13] reported ferromagnetism below 15 K in monatomic-Co chains at the Pt(997) surface step edge. While this system is unlikely to lead to room temperature spintronic applications, it provides a unique opportunity to study both theoretically and experimentally magnetic and transport anisotropies in monatomic ferromagnetic chains. The experiments[13] revealed an unexpectedly strong MAE ($\sim$2.0±0.2 meV/Co atom) with the easy magnetization axis directed along a peculiar angle of 43° towards the Pt step edge and normal to the Co chain.

We analyzed the experiment by considering two possible Pt(111) surface step edge geometries, the $\langle 100 \rangle$ microfaceted A-step and the $\langle 111 \rangle$ microfaceted B-step.[23] In the left inset of Fig. 2 we show model supercells for the B-step that consist of a sub-subsurface and a subsurface Pt layer built of six rows of Pt atoms, while the surface step is modeled by three rows of Pt, one Co row, and two rows of empty Pt sites. Vacuum was modeled by the equivalent of two empty Pt layers. All interatomic distances in the y-z plane were relaxed using scalar-relativistic atomic forces.[24] This represents an important improvement over previous calculations,[14,15] which assumed values for pure Pt.

The self-consistent relativistic FP-LAPW calculations were performed for magnetization aligned along the z axis, using 180 k-points in a quasi-2D BZ. The MAE is shown in Fig. 2. As already described in Ref. 14, the step-edge removes any high-symmetry directions in the y-z plane. The easy axis is tilted from the z axis towards the Pt step edge by
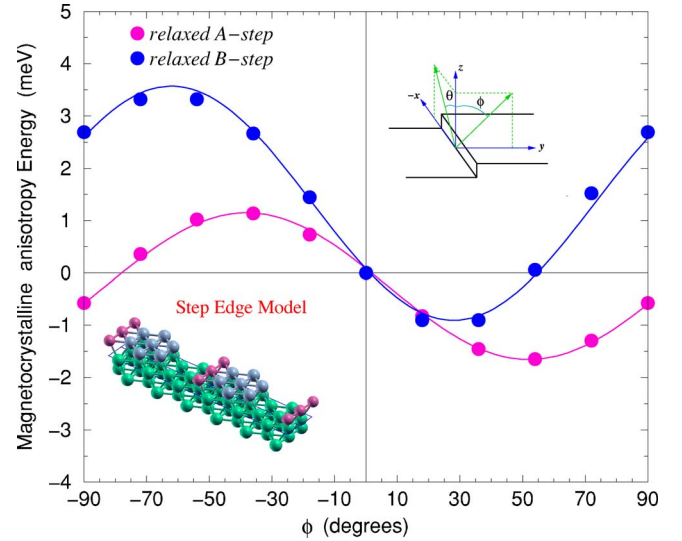

FIG. 2. (Color online) Monatomic-Co chain, MAE as a function of the magnetization angle ϕ. Solid lines are fits to the numerical points $[1.145-2.801\cos^2(\phi-52°)]$ eV (*A-step*) and $[3.530-4.474\cos^2(\phi-28°)]$ eV (*B-step*). Left inset, schematic crystal structure, used to represent the Co chain at the Pt(111) surface B-step edge. Right inset, polar angles ϕ and θ.

52° for the A-step and by 28° for the B-step, in good agreement with the experimentally observed[13] angle of 43°. The total energy difference between states with the magnetization along the hard and easy axes is $\approx$2.8 meV/Co (A-step) and 4.5 meV/Co (B-step); the experimental value of $\sim$2 meV/Co was obtained from magnetic reversal measurements at temperature 45 K. Higher experimental MAE and therefore even better quantitative agreement between our calculations and experiment is expected at temperatures below the ferromagnetic transition temperature in this system.

The energy differences between states with M_S along the x axis (along the Co chain) or y axis (in-plane, perpendicular to the chain), and the z axis (out-of-plane, perpendicular to the chain) are shown in Table II. For the A-step, the MAE is

TABLE II. The MAE and DOS in monatomic-Co chain: Total energy differences $E_x - E_z$, $E_y - E_z$ (meV), integral DOS ($N_I(E_F)$, 1/eV) for $\vec{M}_s \| x, y$, and z axes, and magnetocrystalline anisotropy constants (meV).

	$\vec{M}_S \| x$ axis	$\vec{M}_S \| y$ axis	$\vec{M}_S \| z$ axis
A-step $E_{x,y} - E_z$	8.54	−0.571	
$N_I(E_F)$	26.225	24.963	24.719
B-step $E_{x,y} - E_z$	−0.190	2.639	
$N_I(E_F)$	24.731	29.313	26.606
Anisotropy constants	K_1	K_2	K_3
Relaxed A-step	−1.99	2.28	1.16
Relaxed B-step	−0.63	−0.71	−2.00
Unrelaxed B-step (Ref. 14)	−1.70	−0.12	−1.34
Unrelaxed B-step (Ref. 15)	−0.16	−1.06	−4.81

relatively weak in the y-z plane, and it becomes very strong when M_S is rotated towards the x axis. For the B-step, the MAE is stronger in y-z plane, and becomes weaker for x-z plane. Furthermore, we can evaluate the magnetic anisotropy constants by fitting our results to the total energy angular dependence,[15] $[K_1\cos 2\theta + K_2(1-\cos 2\theta)\cos 2\phi + K_3\sin 2\theta \sin \phi]$, where $K_{1,2,3}$ are the uniaxial anisotropy constants, and θ and ϕ are conventional polar angles. The calculated values of the anisotropy constants are shown in Table II and compared with previous results assuming no structural relaxation.[14,15] The Co-chain anisotropy constants, ~2 meV/Co, set a record, exceeding the bulk and surface anisotropies for the conventional transitional metal materials. Similarly, the anisotropy in N_I is large. For the A-step, e.g., we obtained a (6.1%) anisotropy in the integral DOS, indicating a sizable TAMR effect. Note that for the one-dimensional chain we can make an alternative estimate of the magnitude of the TAMR based on the calculated difference between the number of energy bands at E_F for the two M_S directions. We obtained 25 bands for M_S along the z axis and 26 bands for M_S parallel to the x axis. The corresponding 4% effect is consistent with the estimate based on the calculated DOS anisotropies. For the B-step, the change in N_I for different magnetization orientations is particularly large for M_S along the x and y axes. The corresponding DOS anisotropy is 18.5%.

To conclude, our theoretical results for DOS and magnetocrystalline anisotropies in CoPt structures, based for both quantities on the same *ab initio* relativistic band structures and in the latter one agreeing quantitatively with available experimental data, suggest sizable TAMR effects in these metal ferromagnets. While the anisotropies in the ferromagnetic material make the TAMR possible, the magnitude of the effect can be very sensitive to parameters of the entire tunnel device, most notably of the geometry and crystalline quality of the tunnel junction, as demonstrated in $(Ga,Mn)As$ based devices.[9,10] The integral DOS anisotropies calculated here for the CoPt systems are larger than their $(Ga,Mn)As$ counterparts.

[1] T. Dietl, in *Advances in Solid State Physics*, edited by B. Kramer (Springer, Berlin, 2003), p. 413.

[2] I. Zutic, J. Fabian, and S. D. Sarma, Rev. Mod. Phys. **76**, 323 (2004).

[3] T. Jungwirth, Q. Niu, and A. H. MacDonald, Phys. Rev. Lett. **88**, 207208 (2002).

[4] M. Onoda and N. Nagaosa, J. Phys. Soc. Jpn. **71**, 19 (2002).

[5] T. Jungwirth, J. Sinova, K. Wang, K. W. Edmonds, R. P. Campion, B. L. Gallagher, C. T. Foxon, Q. Niu, and A. H. MacDonald, Appl. Phys. Lett. **83**, 320 (2003).

[6] T. Dietl, F. Matsukura, H. Ohno, J. Cibert, and D. Ferrand, in *Recent Trends in Theory of Physical Phenomena in High Magnetic Fields*, edited by I. Vagner (Kluwer, Dordrecht, 2003), p. 197.

[7] Y. Yao, L. Kleinman, A. H. MacDonald, J. Sinova, T. Jungwirth, Ding-sheng Wang, Enge Wang, and Qian Niu, Phys. Rev. Lett. **92**, 037204 (2004).

[8] C. Gould, C. Ruster, T. Jungwirth, E. Girgis, G. M. Schott, R. Giraud, K. Brunner, G. Schmidt, and L. W. Molenkamp, Phys. Rev. Lett. **93**, 117203 (2004).

[9] C. Ruster, C. Gould, T. Jungwirth, J. Sinova, G. M. Schott, R. Giraud, K. Brunner, G. Schmidt, and L. W. Molenkamp, Phys. Rev. Lett. **94**, 027203 (2005).

[10] A. D. Giddings, M. N. Khalid, T. Jungwirth, J. Wunderlich, S. Yasin, R. P. Campion, K. W. Edmonds, J. Sinova, K. Ito, K. Y. Wang, D. Williams, B. L. Gallagher, and C. T. Foxon, Phys. Rev. Lett. **94**, 127202 (2005).

[11] A. Yermakov and V. Maykov, Phys. Met. Metallogr. **69**, 198 (1990).

[12] A. B. Shick and O. N. Mryasov, Phys. Rev. B **67**, 172407 (2003).

[13] P. Gambardella, A. Dallmeyer, K. Maiti, M. C. Malagoli, W. Eberhardt, K. Kern, and C. Carbone, Nature (London) **416**, 301 (2002).

[14] A. B. Shick, F. Máca, and P. M. Oppeneer, Phys. Rev. B **69**, 212410 (2004).

[15] B. Újfalussy, B. Lazarovits, L. Szunyogh, G. M. Stocks, and P. Weinberger, Phys. Rev. B **70**, 100404(R) (2004).

[16] D. J. Singh, *Planewaves, Pseudopotentials and the LAPW Method* (Kluwer Academic, Boston, 1994), p. 115.

[17] A. B. Shick, D. L. Novikov, and A. J. Freeman, Phys. Rev. B **56**, R14259 (1997).

[18] A. I. Lichtenstein, M. I. Katsnelson, V. P. Antropov, and V. A. Gubanov, J. Magn. Magn. Mater. **67**, 65 (1987).

[19] W. E. Pickett, H. Krakauer, and P. B. Allen, Phys. Rev. B **38**, 2721 (1988).

[20] M. Lehmann and M. Taut, Phys. Status Solidi B **54**, 469 (1972).

[21] M. B. Stearns, in *3d, 4d, and 5d Elements, Alloys and Compounds*, edited by H. P. J. Wijn, Landolt-Bornstein, New Series, Group III (Springer, Berlin, 1986), Vol. 19, p. 34.

[22] I. I. Mazin, Phys. Rev. Lett. **83**, 1427 (1999).

[23] G. Boisvert, L. J. Lewis, and M. Scheffler, Phys. Rev. B **57**, 1881 (1998).

[24] F. Máca, A. B. Shick, and J. Redinger, Czech. J. Phys. (to be published).